

FUTURE  
CIRCULAR  
COLLIDER

# FCC-ee Higgs CP Study

**Nicholas Pinto** (JHU), **Andrei Gritsan** (JHU), **Jan Eysermans** (MIT), **Valdis Slokenbergs** (JHU)

[Second Annual U.S. Future Circular Collider \(FCC\) Workshop](#)

**26 March 2024**



**Massachusetts  
Institute of  
Technology**



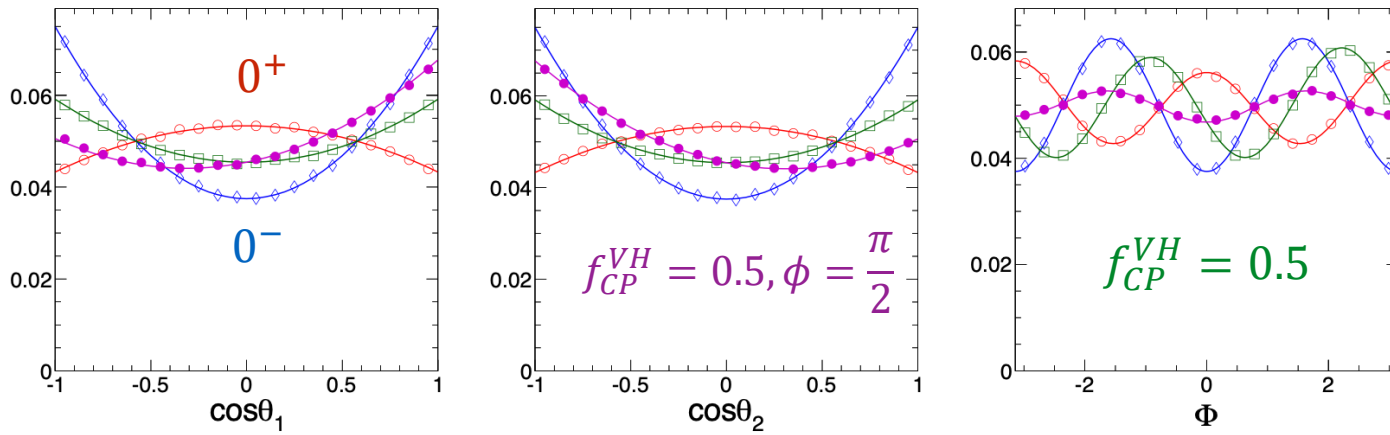
# Outline:

- Overview of Past Studies
- Current Study:
  - Selection and Efficiency
  - Results
- MELA
  - Reweighting in the FCC Framework
  - Future Avenues



# Past Studies: Snowmass 2013

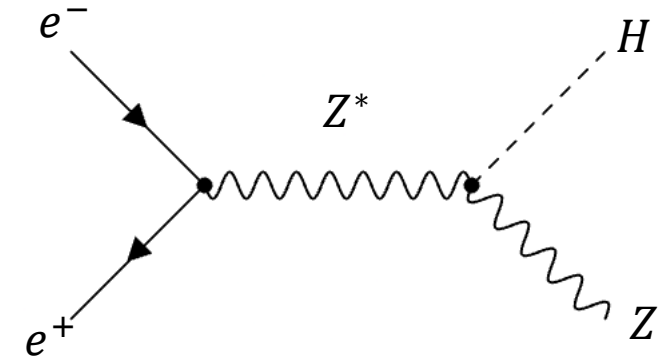
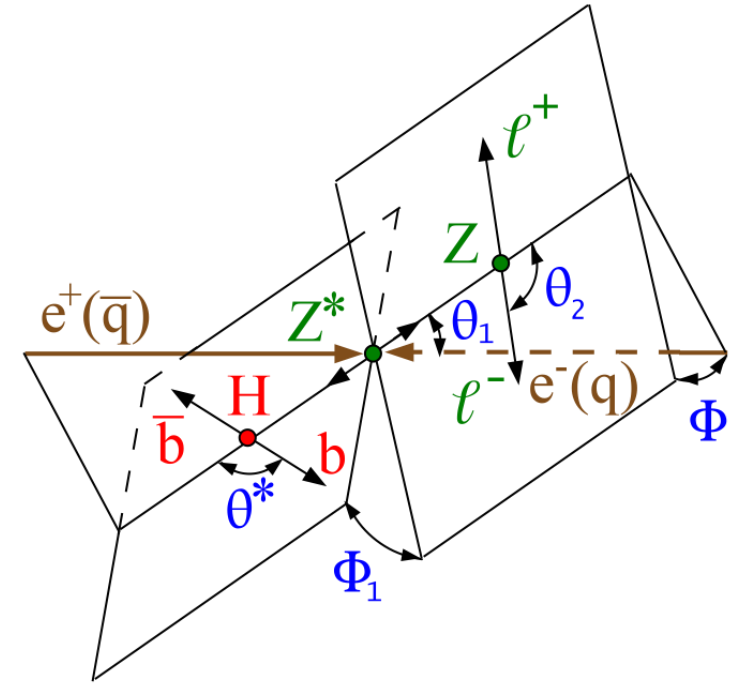
[arXiv:1309.4819](https://arxiv.org/abs/1309.4819)



$$A(H \rightarrow V_1 V_2) = v^{-1} \left( a_1^{HVV} m_V^2 \epsilon_1^* \epsilon_2^* + a_2^{HVV} f_{\mu\nu}^{*(1)} f^{*(2),\mu\nu} + a_3^{HVV} f_{\mu\nu}^{*(1)} \tilde{f}^{*(2),\mu\nu} \right)$$

$$f_{CP}^{HX} \equiv \frac{\Gamma_{H \rightarrow X}^{CP \text{ odd}}}{\Gamma_{H \rightarrow X}^{CP \text{ odd}} + \Gamma_{H \rightarrow X}^{CP \text{ even}}}$$

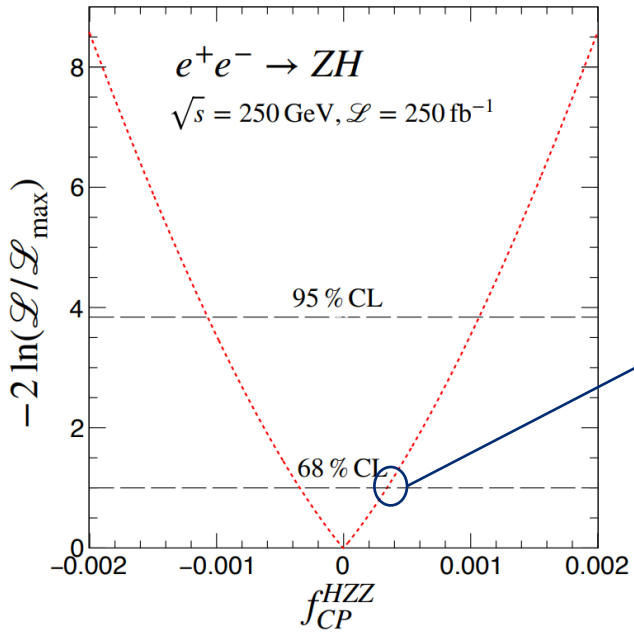
$$f_{CP}^{HVV} = \frac{|a_3^{HVV}|^2}{\sum |a_i^{HVV}|^2 (\sigma_i^{HVV} / \sigma_3^{HVV})}$$





# Past Studies: Snowmass 2022

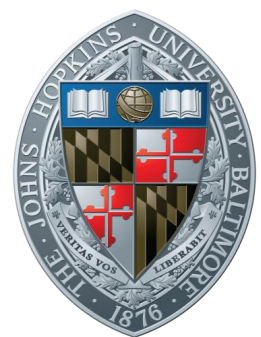
[arXiv:2205.07715](https://arxiv.org/abs/2205.07715)



| E (GeV) | $\mathcal{L}$ (fb $^{-1}$ ) | $f_{CP}^{HVV}$          |
|---------|-----------------------------|-------------------------|
| 250     | 250                         | $\pm 3.4 \cdot 10^{-4}$ |
| 250     | 2,500                       | $\pm 3.9 \cdot 10^{-5}$ |
| 350     | 350                         | $\pm 1.2 \cdot 10^{-4}$ |
| 350     | 3,500                       | $\pm 2.9 \cdot 10^{-5}$ |
| 500     | 500                         | $\pm 4.3 \cdot 10^{-5}$ |
| 500     | 5,000                       | $\pm 1.3 \cdot 10^{-5}$ |
| 1,000   | 1,000                       | $\pm 1.0 \cdot 10^{-5}$ |
| 1,000   | 10,000                      | $\pm 3.0 \cdot 10^{-6}$ |

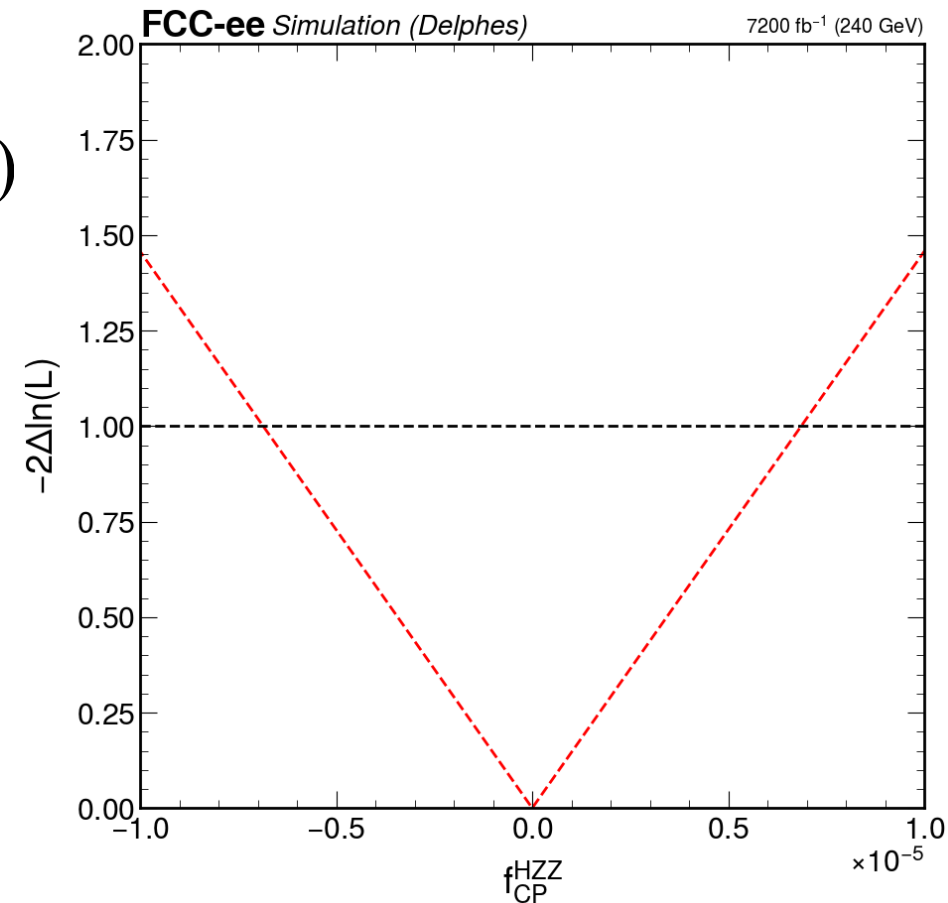
| collider | energy  | $\int \mathcal{L} dt$ (fb $^{-1}$ ) | production                       | $\sigma$ (fb) | decay  | $\sigma \times \mathcal{B}$ (fb) | $N_{\text{prod}}$ | $N_{\text{reco}}$ | $f_{\text{jet}}$ |
|----------|---------|-------------------------------------|----------------------------------|---------------|--|----------------------------------|-------------------|-------------------|------------------|
| pp       | 14 TeV  | 3000                                | $gg \rightarrow H$               | 49850         | $H \rightarrow ZZ^* \rightarrow 4\ell$           | 6.23                             | 18694             | 5608              | 0.1              |
| pp       | 14 TeV  | 3000                                | $V^*V^* \rightarrow H$           | 4180          | $H \rightarrow ZZ^* \rightarrow 4\ell$           | 0.52                             | 1568              | 470               | 0.6              |
| pp       | 14 TeV  | 3000                                | $W^* \rightarrow WH$             | 1504          | $H \rightarrow ZZ^* \rightarrow 4\ell$           | 0.19                             | 564               | 169               | 0.5              |
| pp       | 14 TeV  | 3000                                | $Z^* \rightarrow ZH$             | 883           | $H \rightarrow ZZ^* \rightarrow 4\ell$           | 0.11                             | 331               | 99                | 0.5              |
| pp       | 14 TeV  | 3000                                | $t\bar{t} \rightarrow t\bar{t}H$ | 611           | $H \rightarrow ZZ^* \rightarrow 4\ell$           | 0.08                             | 229               | 69                | 1.0              |
| pp       | 14 TeV  | 3000                                | $V^*V^* \rightarrow H$           | 4180          | $H \rightarrow \gamma\gamma$                     | 9.53                             | 28591             | 8577              | 0.6              |
| pp       | 14 TeV  | 3000                                | $Z^* \rightarrow ZH$             | 883           | $H \rightarrow b\bar{b}, Z \rightarrow \ell\ell$ | 34.3                             | 102891            | 690               | -                |
| $e^+e^-$ | 250 GeV | 250                                 | $Z^* \rightarrow ZH$             | 240           | $H \rightarrow b\bar{b}, Z \rightarrow \ell\ell$ | 9.35                             | 2337              | 1870              | -                |
| $e^+e^-$ | 350 GeV | 350                                 | $Z^* \rightarrow ZH$             | 129           | $H \rightarrow b\bar{b}, Z \rightarrow \ell\ell$ | 5.03                             | 1760              | 1408              | -                |
| $e^+e^-$ | 500 GeV | 500                                 | $Z^* \rightarrow ZH$             | 57            | $H \rightarrow b\bar{b}, Z \rightarrow \ell\ell$ | 2.22                             | 1110              | 888               | -                |
| $e^+e^-$ | 1 TeV   | 1000                                | $Z^* \rightarrow ZH$             | 13            | $H \rightarrow b\bar{b}, Z \rightarrow \ell\ell$ | 0.51                             | 505               | 404               | -                |
| $e^+e^-$ | 250 GeV | 250                                 | $Z^*Z^* \rightarrow H$           | 0.7           | $H \rightarrow b\bar{b}$                         | 0.4                              | 108               | 86                | -                |
| $e^+e^-$ | 350 GeV | 350                                 | $Z^*Z^* \rightarrow H$           | 3             | $H \rightarrow b\bar{b}$                         | 1.7                              | 587               | 470               | -                |
| $e^+e^-$ | 500 GeV | 500                                 | $Z^*Z^* \rightarrow H$           | 7             | $H \rightarrow b\bar{b}$                         | 4.1                              | 2059              | 1647              | -                |
| $e^+e^-$ | 1 TeV   | 1000                                | $Z^*Z^* \rightarrow H$           | 21            | $H \rightarrow b\bar{b}$                         | 12.2                             | 12244             | 9795              | -                |

**Signal:**  $e^+e^- \rightarrow ZH, Z \rightarrow \ell\ell$  (7.7%),  $H \rightarrow b\bar{b}$  (58%). **Background:**  $e^+e^- \rightarrow ZZ \rightarrow \ell\ell b\bar{b}$ ,  $N_{\text{reco,Background}} \sim 1/10^{\text{th}}$  of **signal**, Z mass, angles input to combine (template fit),  $f_{CP}^{HVV}$  returned at 68% CL.  
 4+ different samples (SM Signal, BSM Signal, Background, SM/BSM Interference) used to produce fits.



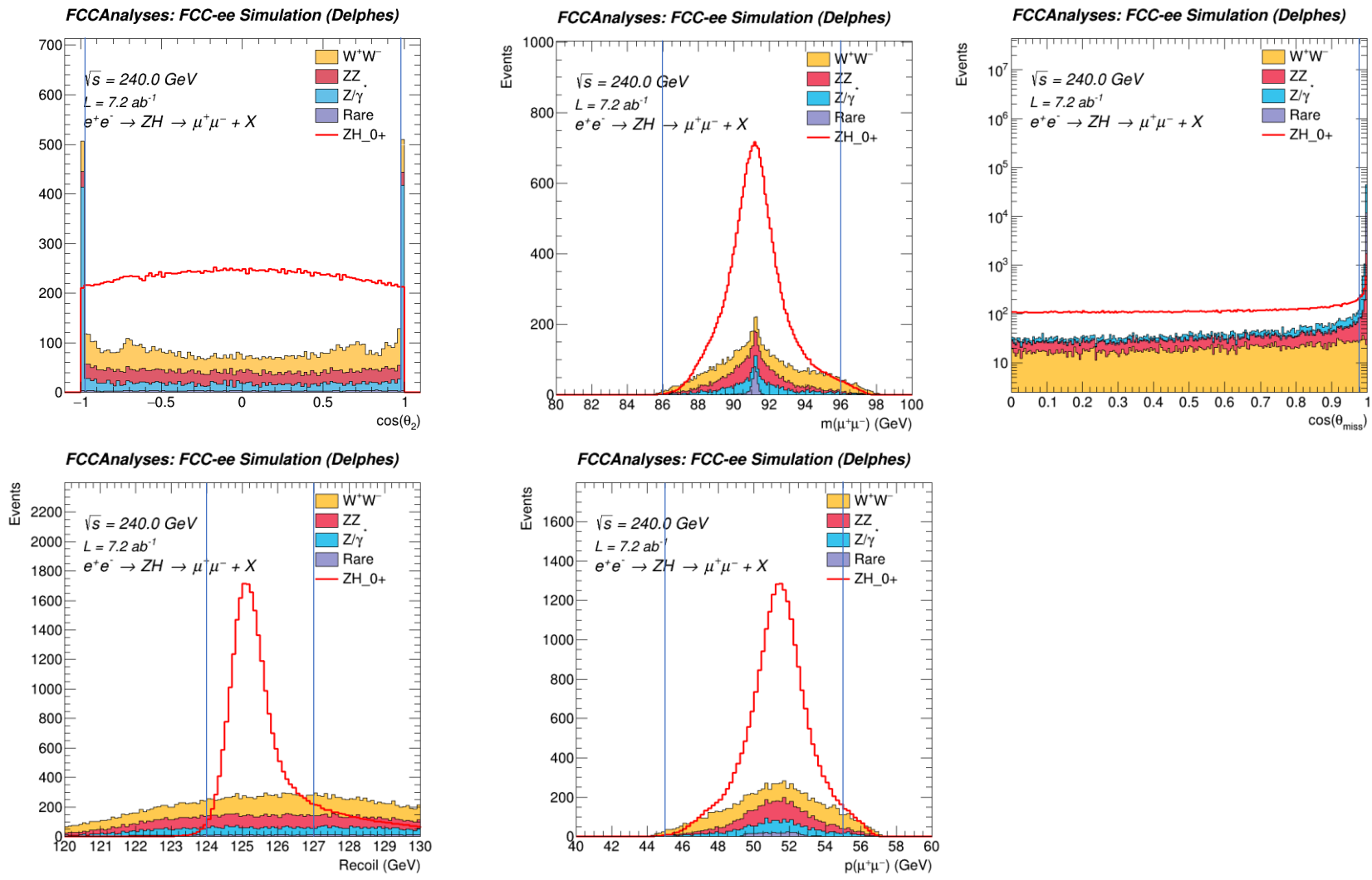
# Overview of Current Study:

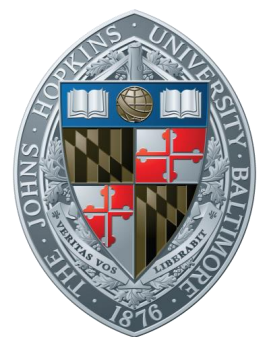
- Target:  $ee \rightarrow ZH, H \rightarrow X$  (recoil),  $Z \rightarrow \mu\mu$  (3.4%)
- Detector simulation uses DELPHES fast sim.
- Template fit made from angular distributions.
- Uses Reco data, FCC signal yield and luminosity.
  - Additional fit w/ Snowmass luminosity used as a comparison.
- Broader range of backgrounds used:
  - Primarily  $WW, ZZ, Z/\gamma^*$





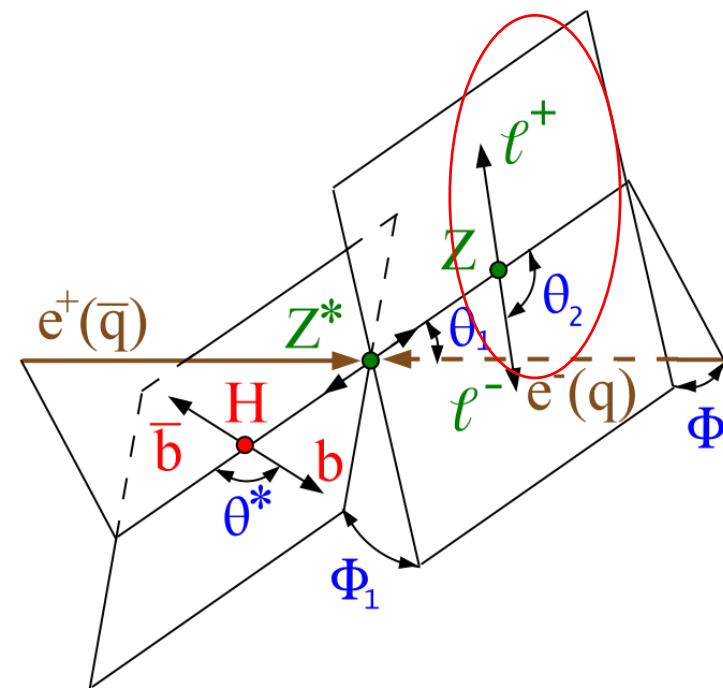
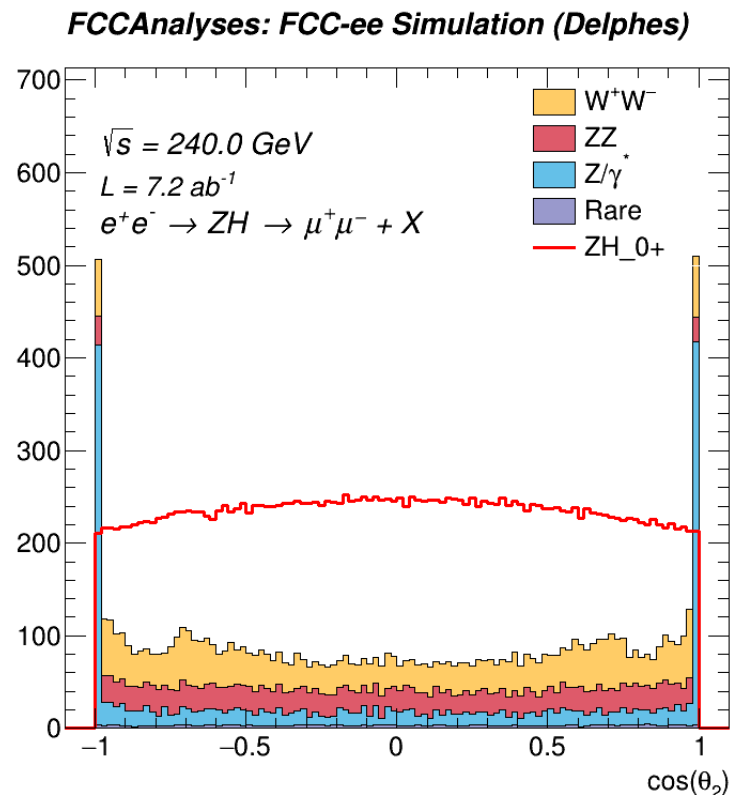
# Current Selection: N-1 Plots:





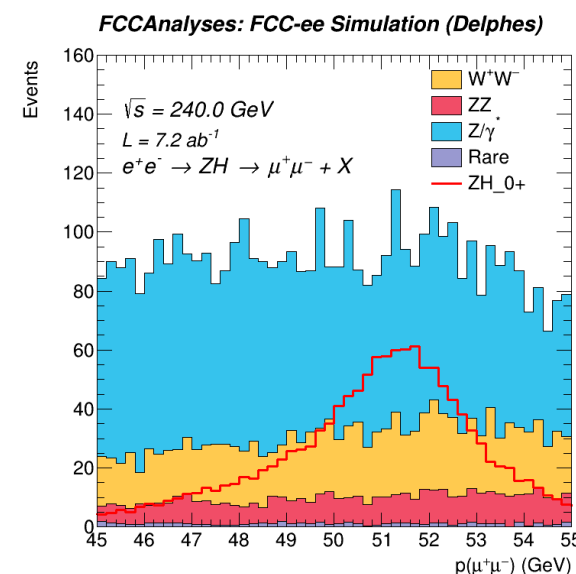
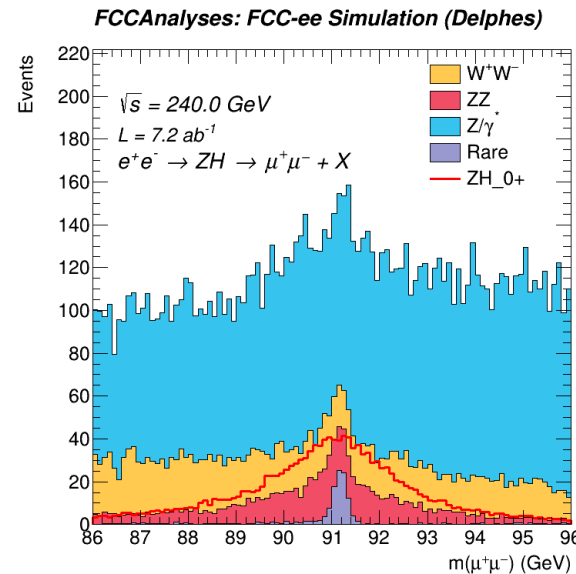
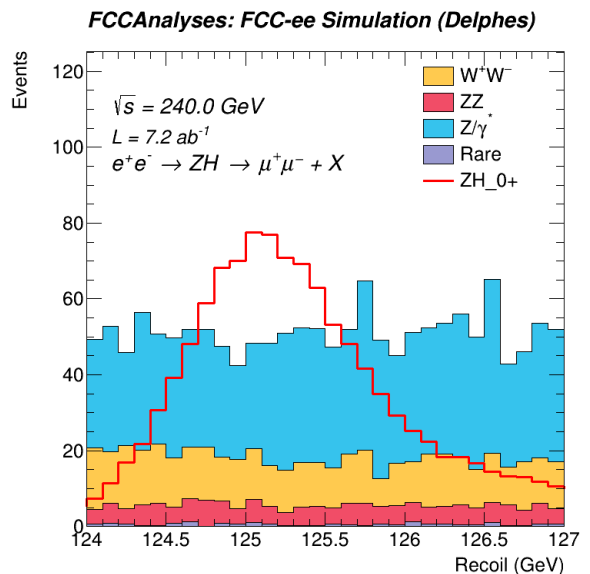
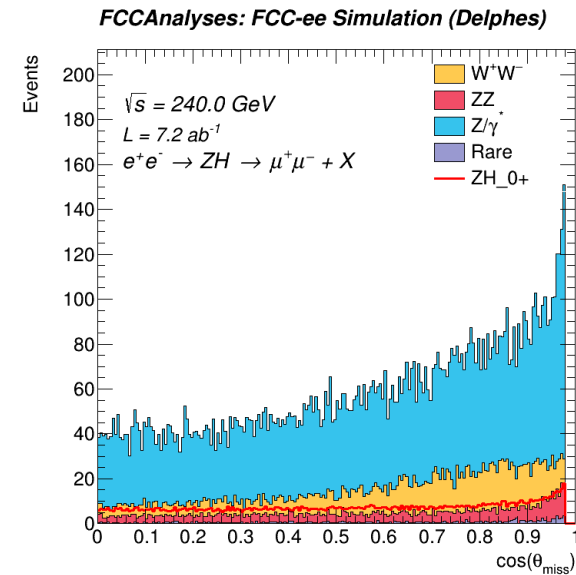
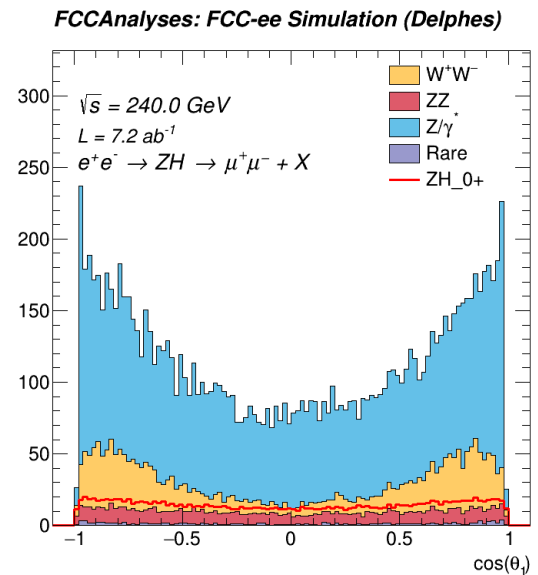
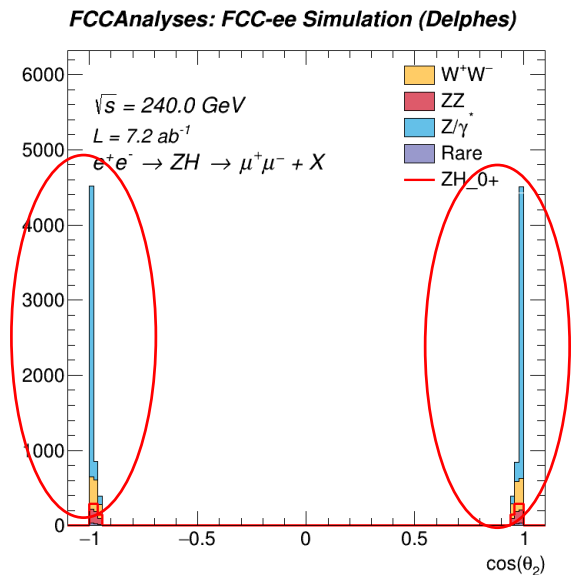
# Selection: Behavior of $\text{Cos } \theta_2$ Endpoints:

- $\text{Cos } \theta_2$  is the angle between muon and recoil direction.
- "Bullhorns" appear at the extrema of  $\text{Cos } \theta_2$  in  $e^+e^- \rightarrow \tau^+\tau^-$





# Events at $\text{Cos } \theta_2$ Endpoints and Correlations to Other Observables:

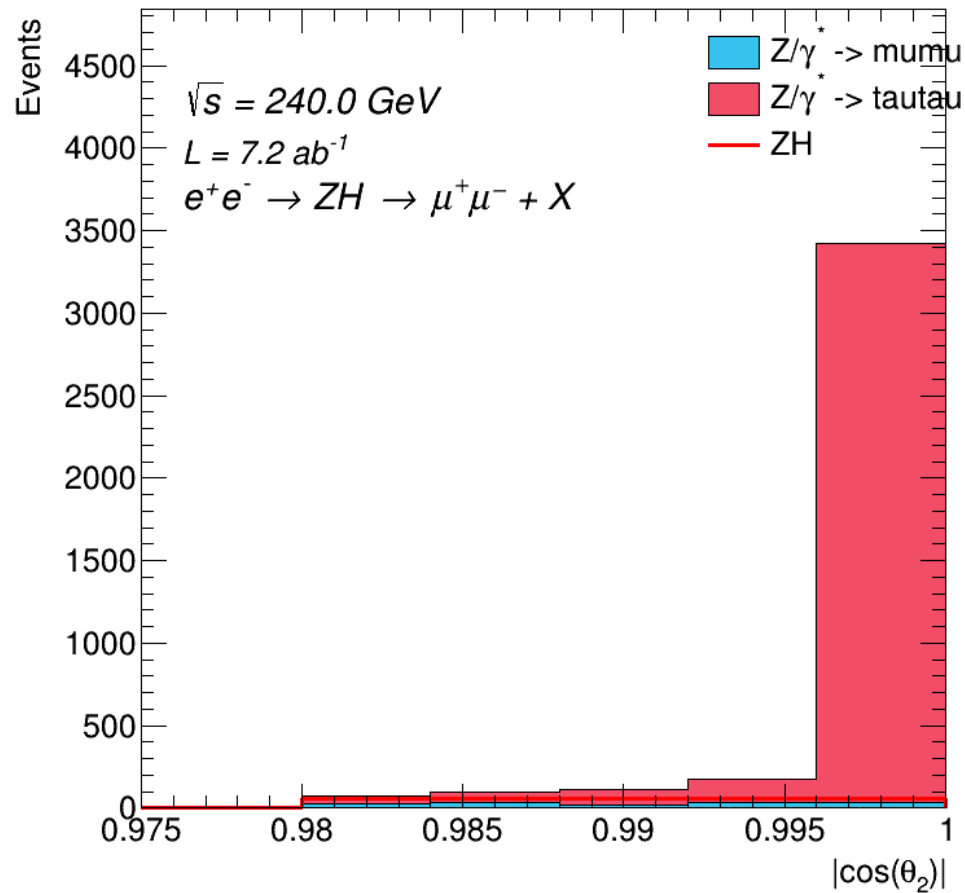




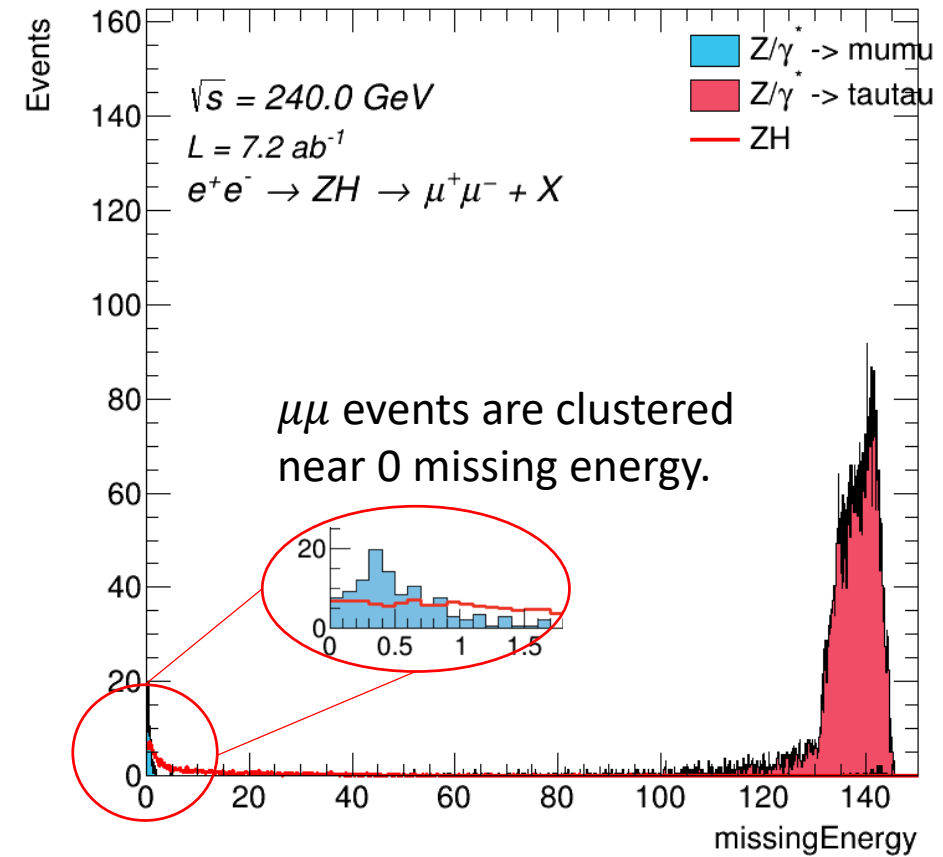


# $\text{Cos } \theta_2$ of $Z/\gamma^* \rightarrow \mu\mu$ and $\tau\tau$ :

FCCAnalyses: FCC-ee Simulation (Delphes)



FCCAnalyses: FCC-ee Simulation (Delphes)

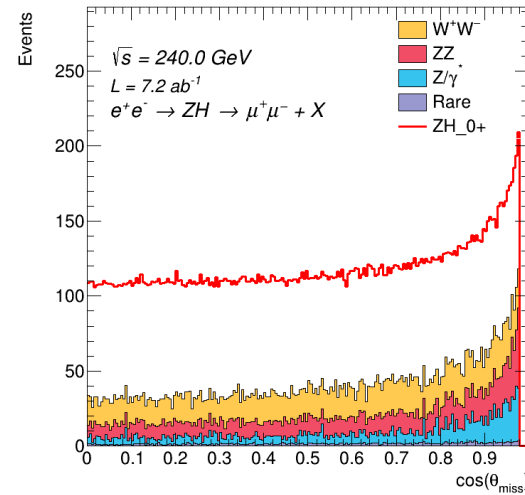


Horns are nearly all from  $\tau\tau$  events. No events in the bins below 0.98.  
Missing energy from  $\tau$  decays into neutrinos.

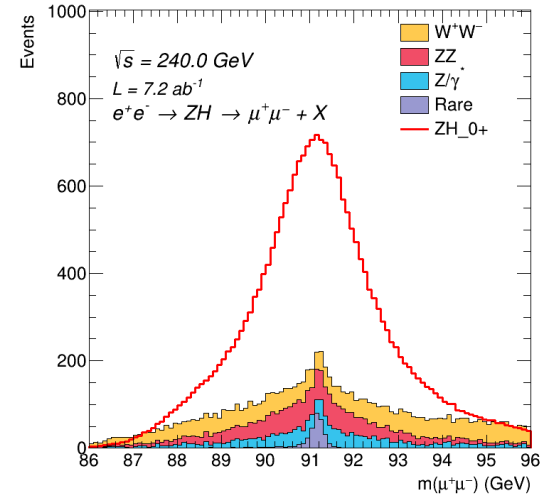


# All Cuts Made:

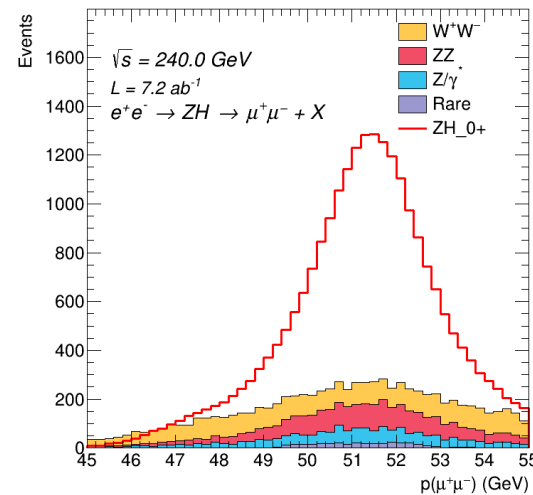
FCCAnalyses: FCC-ee Simulation (Delphes)



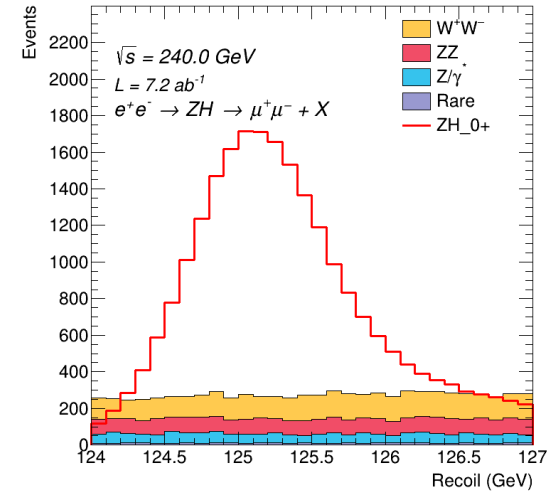
FCCAnalyses: FCC-ee Simulation (Delphes)



FCCAnalyses: FCC-ee Simulation (Delphes)



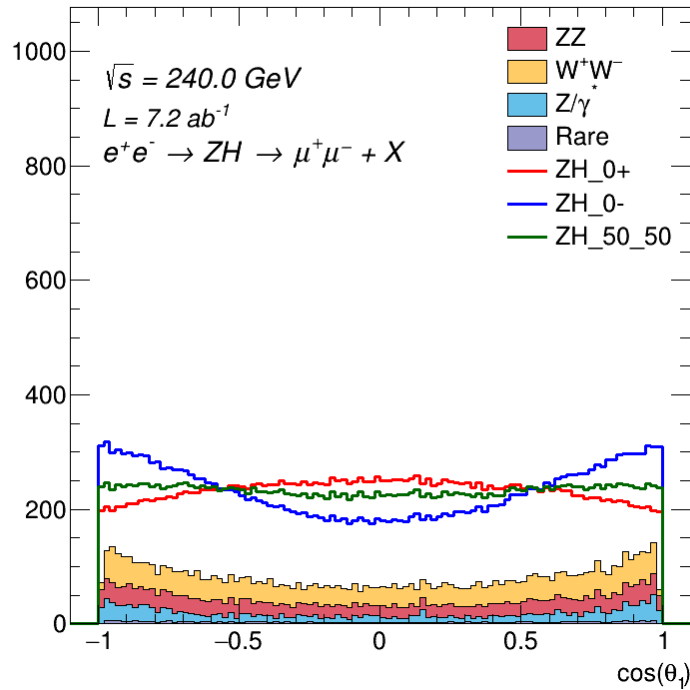
FCCAnalyses: FCC-ee Simulation (Delphes)



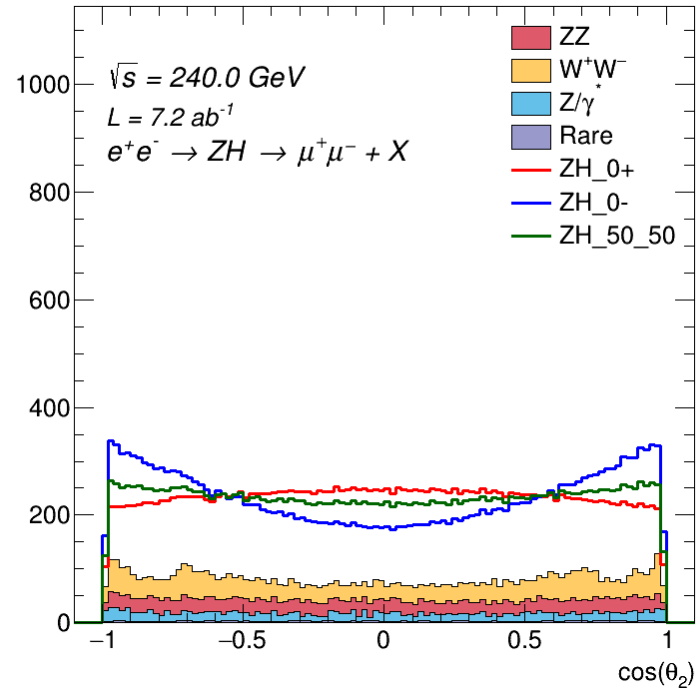


# All Cuts Made: Angular Distributions:

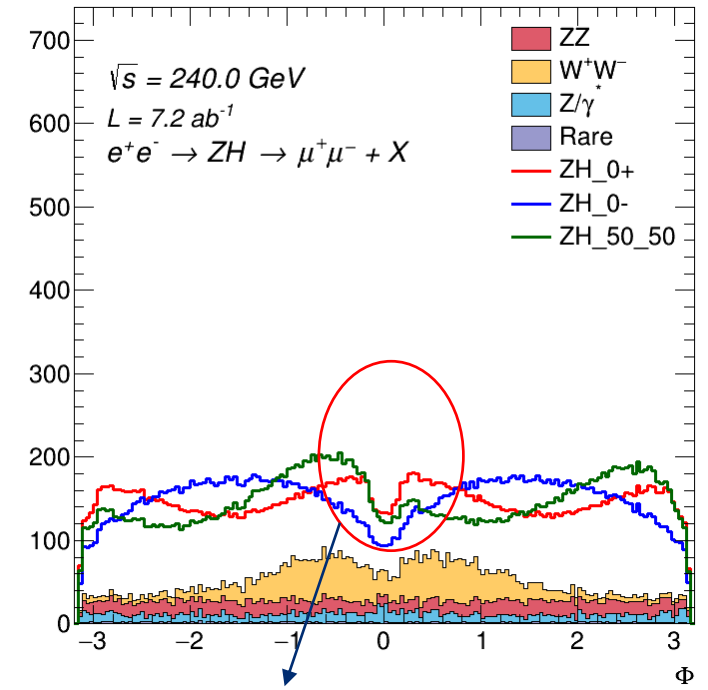
FCCAnalyses: FCC-ee Simulation (Delphes)



FCCAnalyses: FCC-ee Simulation (Delphes)



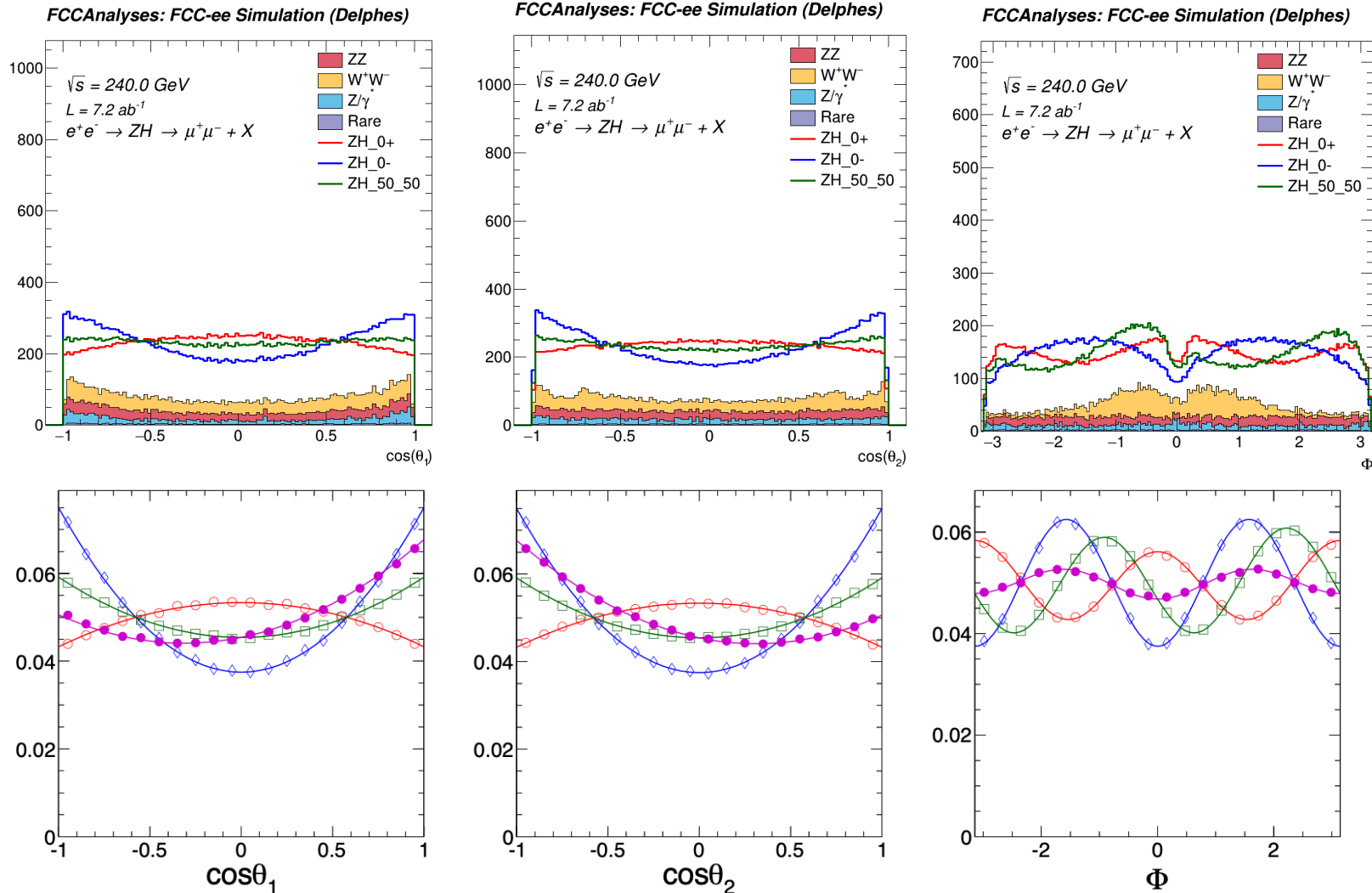
FCCAnalyses: FCC-ee Simulation (Delphes)



Selection effect occurs around  $\Phi = 0$ .



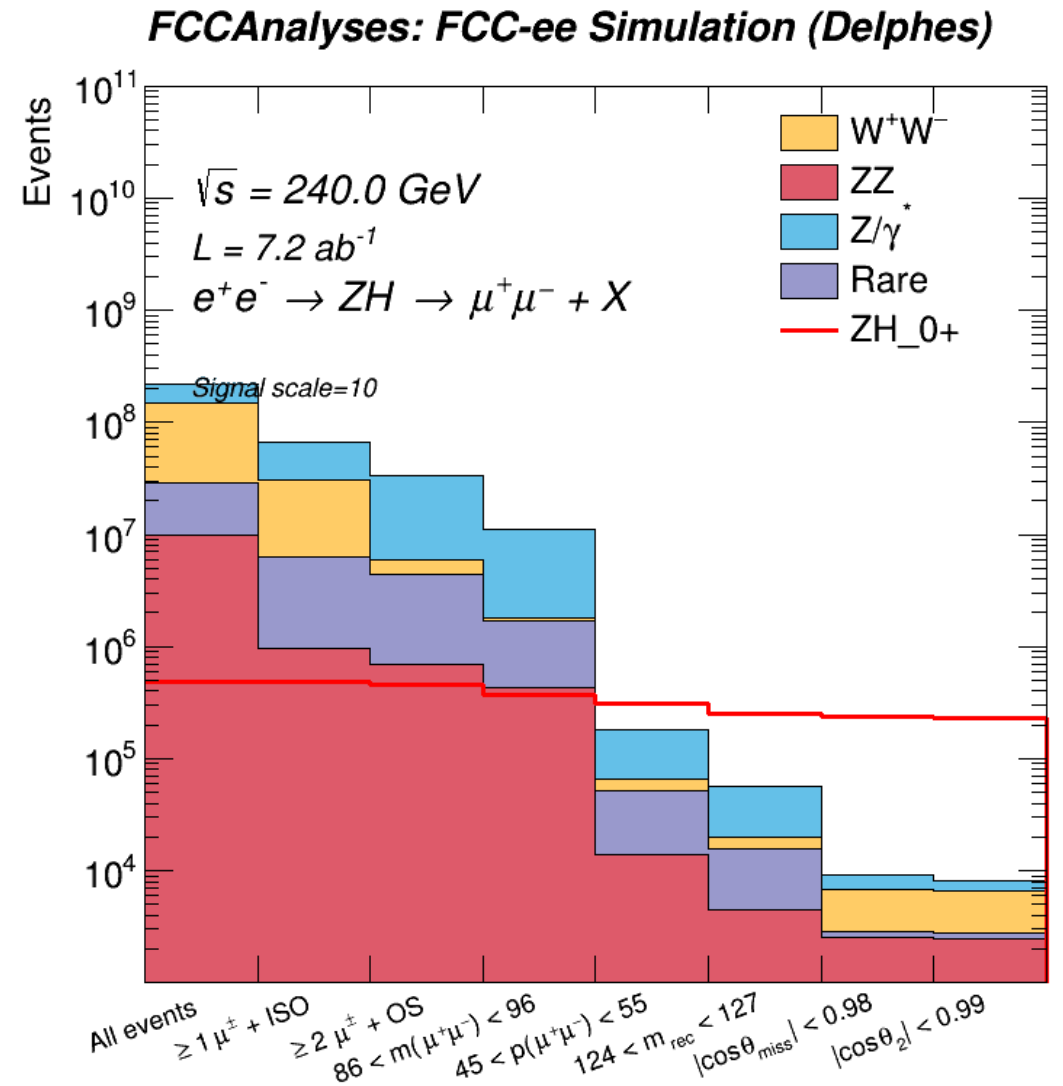
# Comparing Angular Distributions to Snowmass Study:





# Cut Flow:

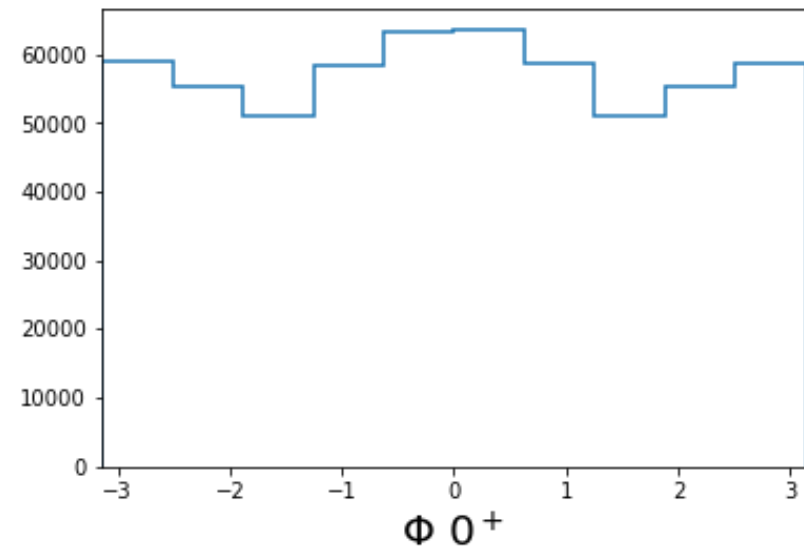
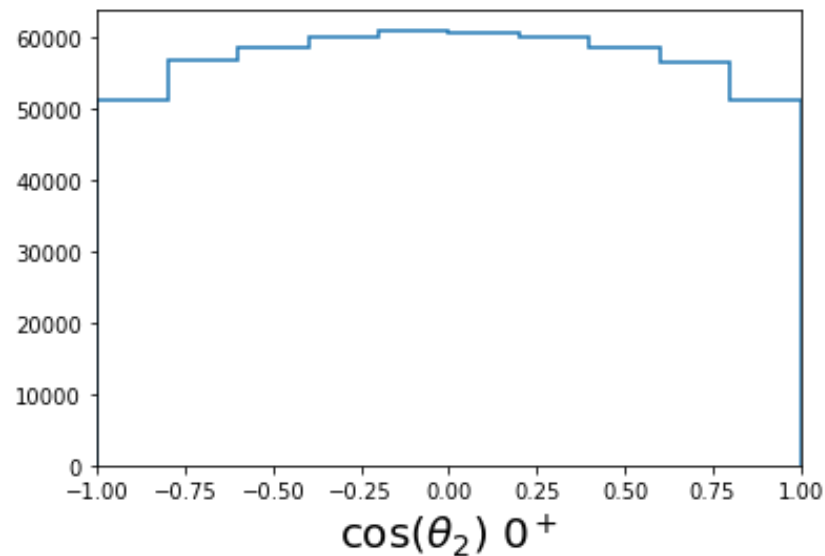
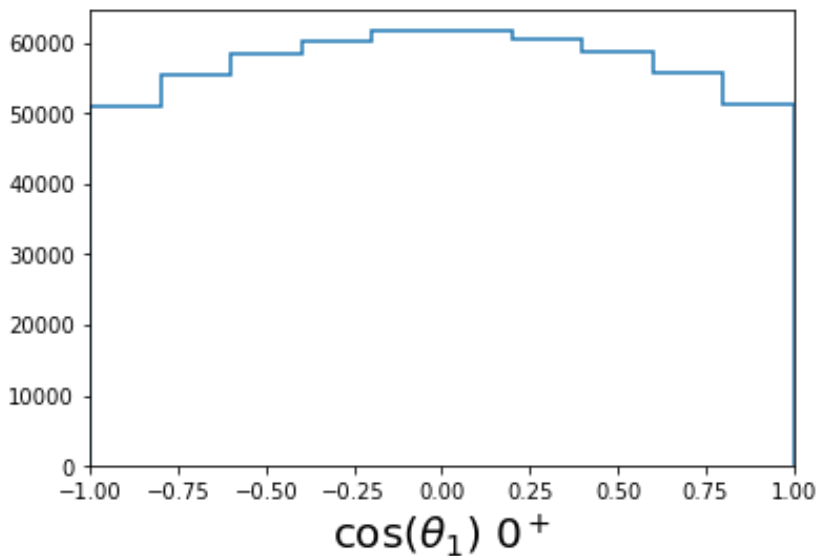
- Signal Selection Efficiency  $\sim 47.9\%$
- Signal : Background  $\sim 2.5$

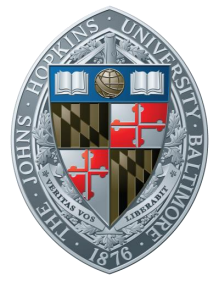




# Template Fit Details:

- 3D histogram filled with 1 angle on each axis.  $\sim 55000$  entries/bin on average.
- 10 bins/axis
- Example projections for  $0^+$  hypothesis:





# Expected Yields After Reco. + Selection:

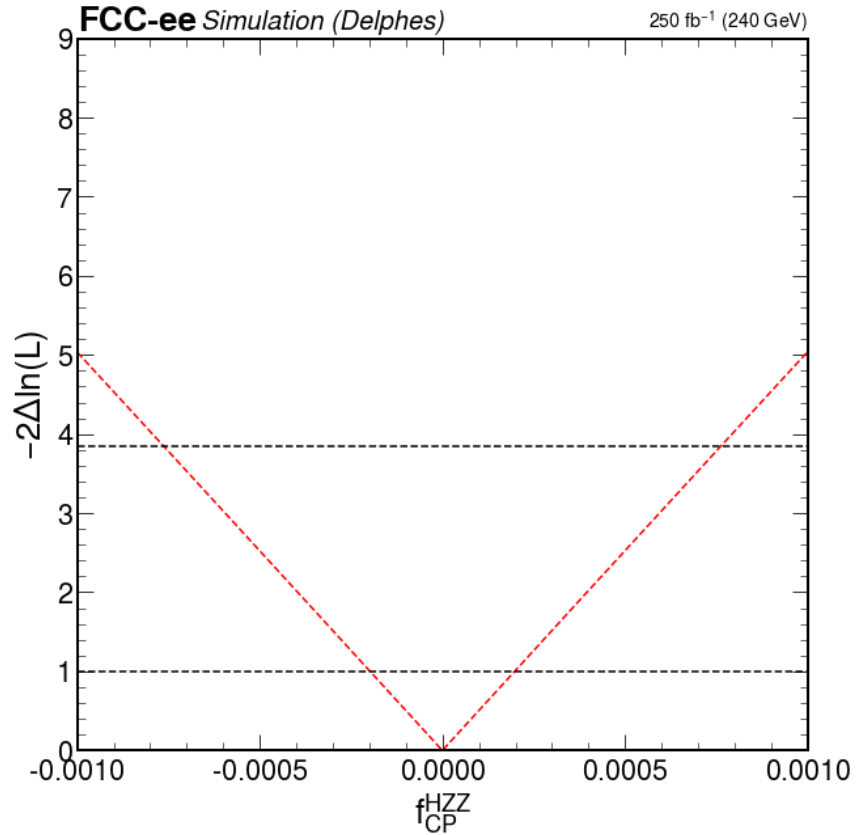
(Red box = signal yields)

| $\int Ldt(fb^{-1})$ | production                               | Yield | $\int Ldt(fb^{-1})$ | production                               | Yield   |
|---------------------|--|-------|---------------------|--|---------|
| 250                 | $ee \rightarrow ZH(0^+)$                 | 809.2 | 7200                | $ee \rightarrow ZH(0^+)$                 | 23303.9 |
| 250                 | $ee \rightarrow ZH(0^-)$                 | 809.3 | 7200                | $ee \rightarrow ZH(0^-)$                 | 23306.6 |
| 250                 | $ee \rightarrow ZH(\text{Positive int})$ | 388.7 | 7200                | $ee \rightarrow ZH(\text{Positive int})$ | 11200.7 |
| 250                 | $ee \rightarrow ZH(\text{Negative int})$ | 389.5 | 7200                | $ee \rightarrow ZH(\text{Negative int})$ | 11238.5 |
| 250                 | $ee \rightarrow WW$                      | 133.7 | 7200                | $ee \rightarrow WW$                      | 3849.9  |
| 250                 | $ee \rightarrow ZZ$                      | 86.1  | 7200                | $ee \rightarrow ZZ$                      | 2480.4  |
| 250                 | $ee \rightarrow \mu\mu$                  | 48.2  | 7200                | $ee \rightarrow \mu\mu$                  | 1388.2  |
| 250                 | $ee \rightarrow \nu\nu Z$                | 11.1  | 7200                | $ee \rightarrow \nu\nu Z$                | 319.3   |
| 250                 | $ee \rightarrow \tau\tau Z$              | 5.0   | 7200                | $ee \rightarrow \tau\tau Z$              | 145.0   |
| 250                 | $e\gamma \rightarrow eZ$                 | 0.0   | 7200                | $e\gamma \rightarrow eZ$                 | 1.1     |
| 250                 | $\gamma e \rightarrow eZ$                | 0.0   | 7200                | $\gamma e \rightarrow eZ$                | 2.1     |
| 250                 | $\gamma\gamma \rightarrow \tau\tau$      | 0.0   | 7200                | $\gamma\gamma \rightarrow \tau\tau$      | 1.4     |



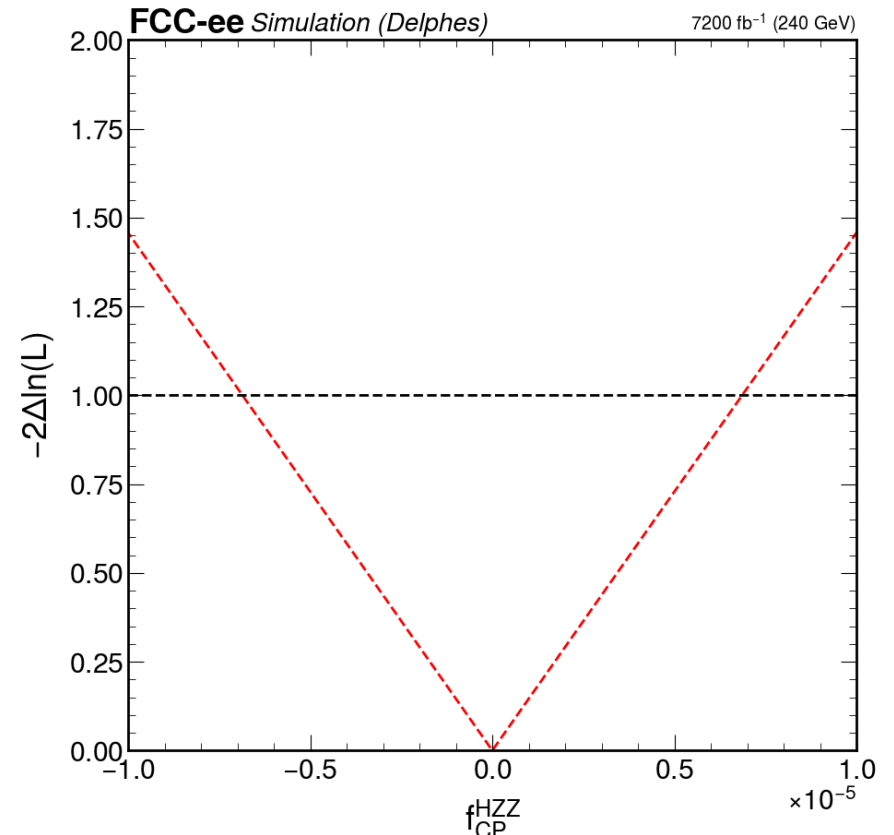
# Fits with Reconstructed Signal $H \rightarrow X, Z \rightarrow \mu\mu$ :

@  $250 fb^{-1}$



68% CL  $\approx \pm 2.0 \text{ E-}4$

@  $7200 fb^{-1}$



68% CL  $\approx \pm 0.7 \text{ E-}5$





# MELA:

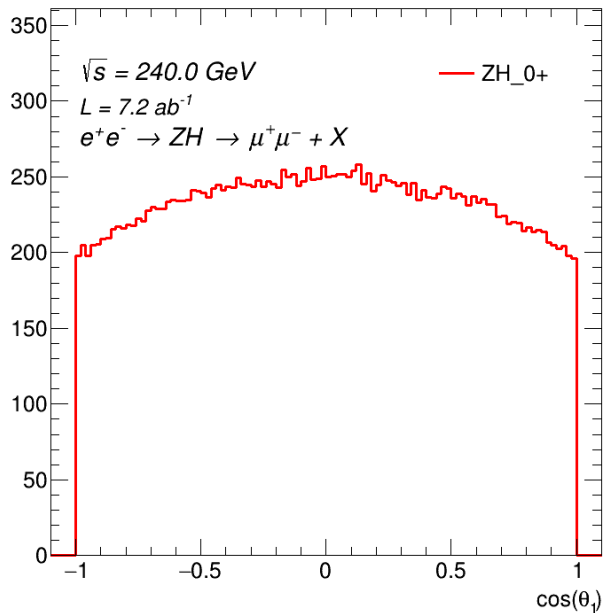
- “Matrix Element Likelihood Approach”
- Calculates transition probability from one hypothesis to another using event kinematics.
  - Used to reweight a distribution in one sample to an alternative hypothesis.
- Calculates angular distributions.
- Currently interfaced to the FCC framework!



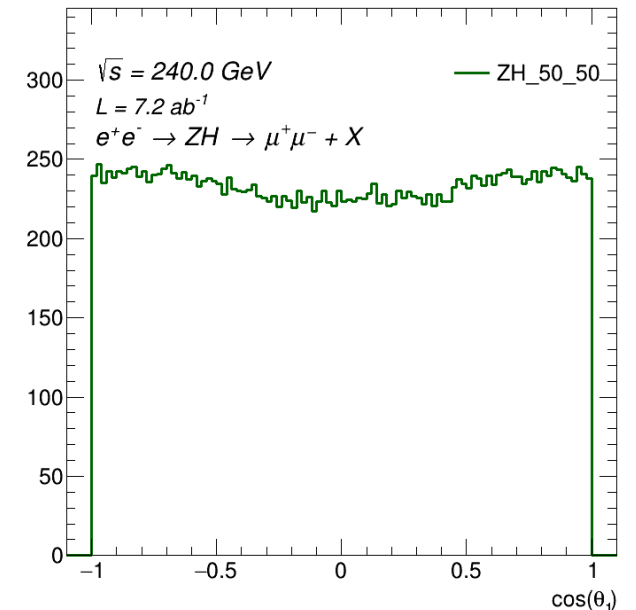
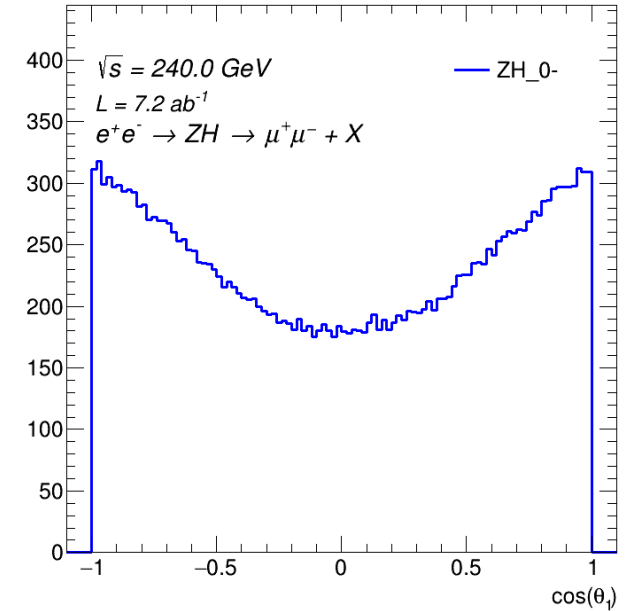
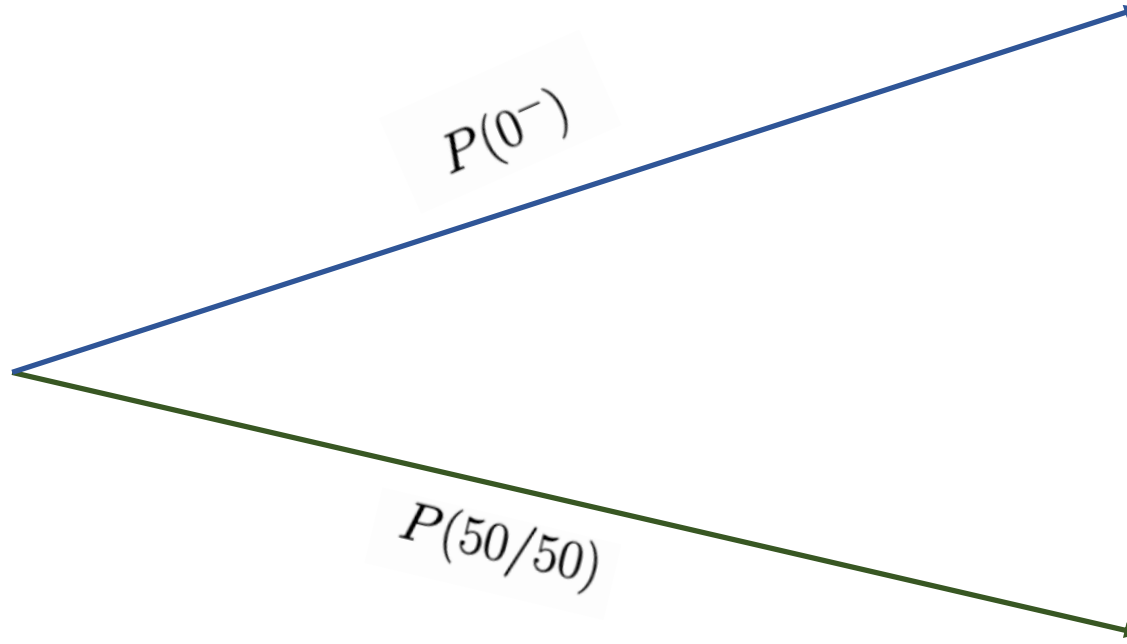
# MELA in this study:

Simulated:

FCCAnalyses: FCC-ee Simulation (Delphes)



Reweighting:



- Angular distributions and probabilities calculated by MELA.
- Reweights  $0^+$  distribution to  $0^-$  and 50/50 mixture distributions.

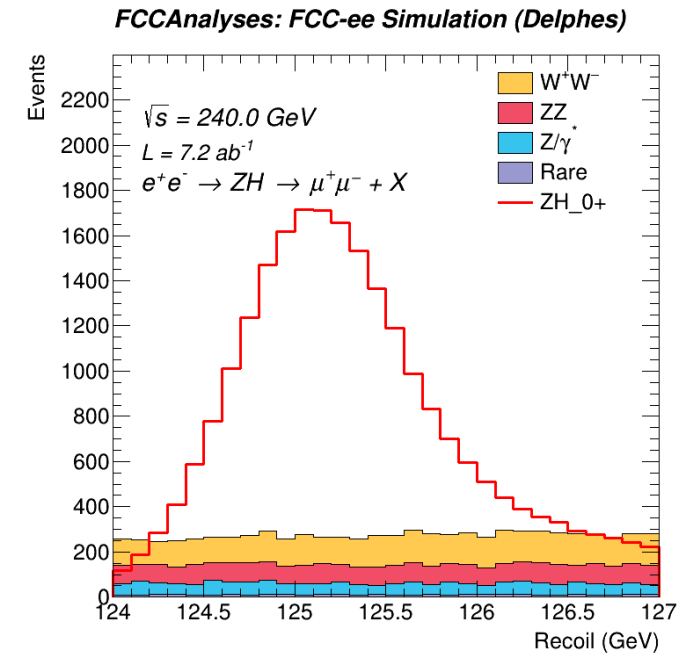
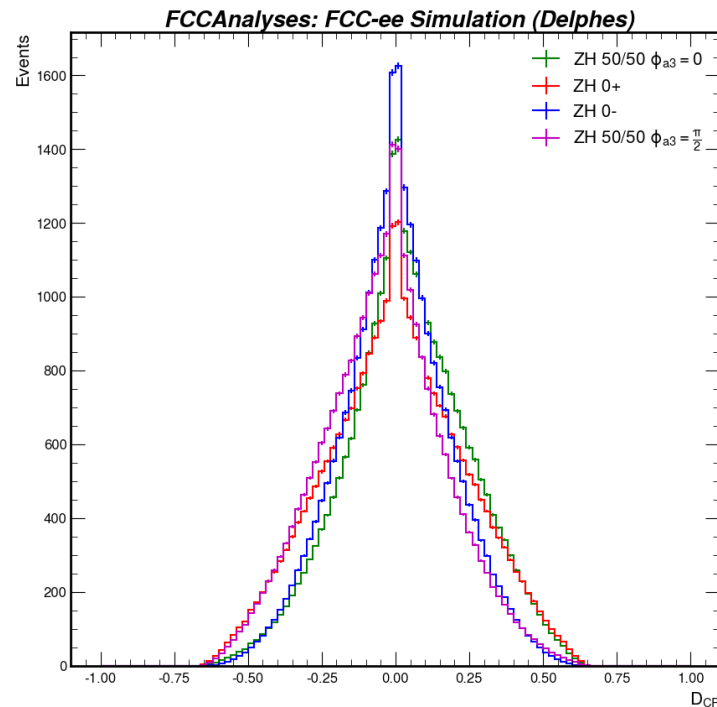
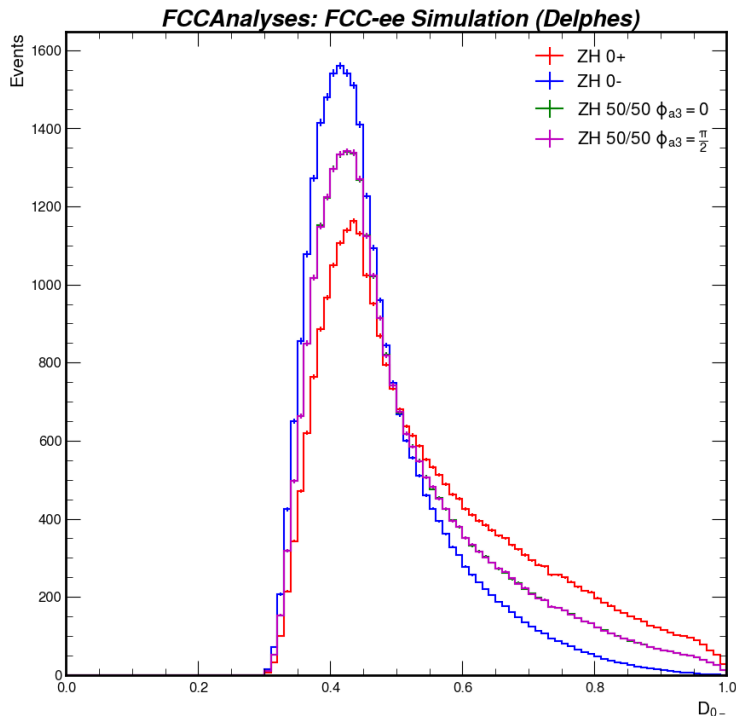


# Improving this study with MELA:

$$D_{0^-} = \frac{P(0^-)}{P(0^+) + P(0^-)}$$

$$D_{CP} = \frac{P(int)}{2\sqrt{P(0^+) * P(0^-)}}$$

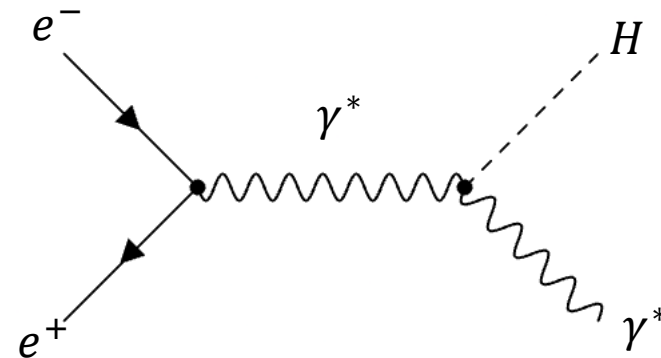
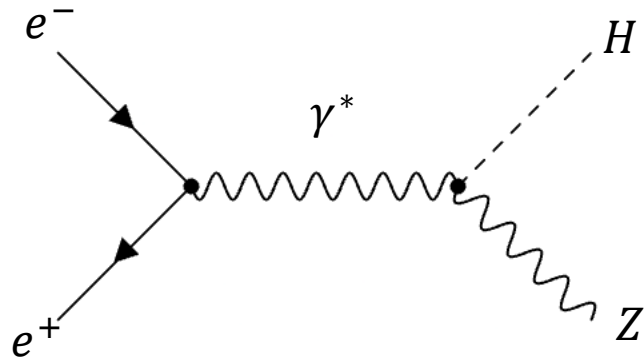
- Discriminants = Optimal observables from MELA probabilities.
- Determine optimal binning, create likelihood fit with  $D_{0^-}$ ,  $D_{CP}$ , and  $m_{rec}$ .





# MELA in future studies:

- MELA can probe couplings besides  $f_{CP}^{HZZ}$ .
  - $f_{CP}^{HZ\gamma^*}$ ,  $f_{CP}^{H\gamma^*\gamma^*}$  studies also possible within FCC framework.





# Conclusions:

- Likelihood fit from angular distributions represents a realistic constraints on  $f_{CP}^{HZZ}$ .
- MELA functional within FCC framework.
  - Pending review to be officially incorporated.
- Update to this study using discriminants in the works!
- Plans to extend this study:
  - $Z \rightarrow e^+e^-$  final state
  - Alternative couplings:  $f_{CP}^{HZ\gamma^*}$ ,  $f_{CP}^{H\gamma^*\gamma^*}$